JINR Summer Student Program 2018

Analog readout for ToF system @NICA

Author:

Dayron Ramos López

Higher Institute of Technologies and Applied Sciences, University of Havana

Supervisors:

Vadim Babkin

Dmitriev Alexandr

Participation period:

1 July-25 August

Summary

1. MPD/NICA Physics

The Nuclotron-based Ion Collider fAcility (NICA) (Fig. 1.1) is an ambitious project still under construction at Joint Institute for Nuclear Research. The NICA global scientific goal is to explore the phase diagram of strongly interacting matter in the region of highly compressed and hot baryonic matter. Such matter exists in neutron stars and in the core of supernova explosions, while in the early Universe we meet the opposite conditions of very high temperature and vanishing baryonic density. In terrestrial experiments, high-density nuclear matter can transiently be created in a finite reaction volume in relativistic heavy ion collisions. In these collisions, a large fraction of the beam energy is converted into newly created hadrons, and new color degrees of freedom may be excited. The properties of excited resonances may noticeably be modified by the surrounding hot and dense medium. At very high temperature or density, this hadron mixture melts and their constituents, quarks and gluons, form a new phase of matter, the quark-gluon plasma. Different phases of strongly interacting matter are shown in the phase diagram of Fig. 1.2. [1].

3

Fig. 1.1. Schematic view of the NICA-Nuclotron complex

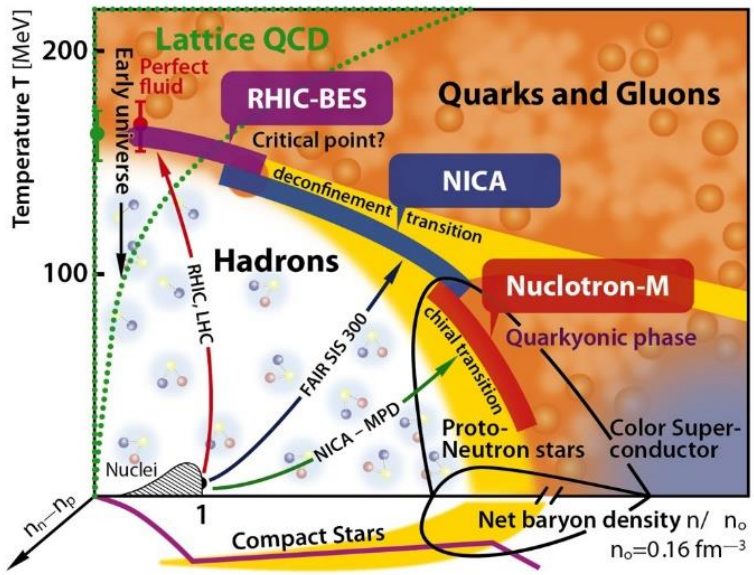

Fig. 1.2. The phase diagram of strongly interacting QCD matter. Phase boundaries, critical end-point, and conjectured dynamical trajectories for an expansion stage are plotted as well.

The project is interested in an intermediate region of the phase diagram, where essential evidence was obtained by the NA49 collaboration within the CERN-SPS energy scan program that the system enters a new phase at a beam energy of about 30 AGeV. The fascinating particularity of this energy range is the critical endpoint located according to the recent lattice QCD calculations at T_E = (162±2) MeV and baryon chemical potential μ_E = (360±40) MeV, whereas model predictions are strongly scattered throughout the regions of $T_E \sim$ 50−170 MeV and $\mu_E \sim$ 200 −1400 MeV [1].

Physics tasks of the NICA heavy-ion program are [2]:

- event-by-event fluctuation in hadron productions (multiplicity, Pt etc.);
- femtoscopic correlation;
- directed and elliptic flows for various hadrons;
- multi-strange hyperon production (including hypernuclei): yield and spectra (the probes of nuclear media phases);
- photon and electron probes;
- charge asymmetry.

The MPD is designed as a 4π-spectrometer capable of detecting charged hadrons, electrons and photons in heavy-ion collisions in the energy range of the NICA collider. To reach this goal, the detector will include a precise 3-D tracking system and a high-performance particle identification system based on time-of-flight measurements and calorimetry. At the design luminosity, the event rate in the MPD interaction region is about 6 kHz; the total charged particle multiplicity exceeds 1000 in the most central Au+Au collisions at $\sqrt{S_{NN}}$= 11 GeV. As the average transverse momentum of the

particles produced in a collision at the NICA energies is below 500 MeV/c, the detector design requires a very low material budget. The general layout of the MPD apparatus is shown in Fig. 1.3.

The Multi-Purpose Detector consists of a barrel part and two endcaps located inside the magnetic field. The barrel part is a shell-like set of various detector systems surrounding the interaction point and aimed at reconstructions and identifying both charged and neutral particles in the pseudorapidity region of $|\eta| \leq 1.3$. The endcaps are aimed at the precise tracking over pseudo rapidity range ($1.3 < |\eta| < 2$). The ion beams interact inside the beam pipe located along the z axis with the central interaction point at $z = 0$ in the center of the detector. The interaction region covers an interval of $|z| \leq 25$ cm.

The barrel part consists of a tracker and particle identification system. The principal tracker is the time projection chamber (TPC) supplemented by the inner tracker (IT) surrounding the interaction region. Both subdetectors (IT and TPC) have to provide precise track finding, momentum determination, vertex reconstruction and pattern recognition [3].

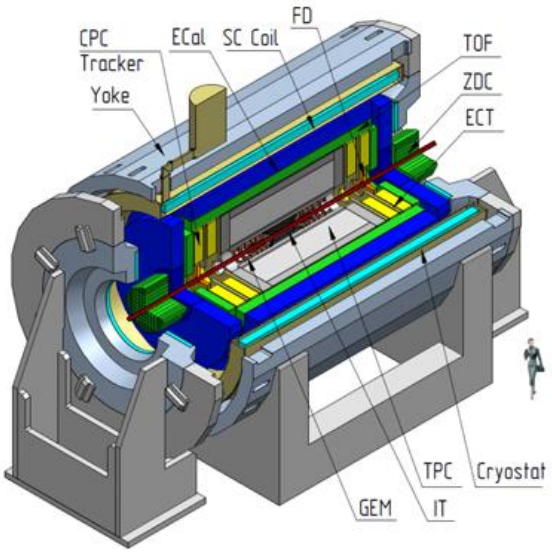

Fig. 1.3. Schematic view of the Multi-Purpose Detector

The event-by-event hadrons identification will provide us with the opportunity to measure, with high statistics, on a single event basis the yields of pions, kaons and protons, their ratios, thus giving a possibility of comprehensive study as many as possible event-by-event dynamical fluctuations and correlations. Consequently, it will provide information on possible instabilities during phase transitions, on the degree of thermal equilibrium, on collective flow phenomena and on expansion dynamics.

Physics goals of the MPD [3] require particle identification over as large as possible phase space volume. The MPD has two main identification subsystems. The first subsystem is high performance time-of-flight (ToF) detector. The ToF together with the TPC must be able to identify

charged hadrons and nuclear clusters in the broad rapidity range and up to total momentum of 3 GeV/c. The fast forward detectors (FD) will provide the ToF system with the start signal. The second PID system is the electromagnetic calorimeter. Its main goal is to identify electrons, photons and measure their energy with high precision.

2. The MPD and BM@N TOF system design

The choice for the TOF system was the Multigap Resistive Plate Chambers (MRPC) with triple stack and strip readout [3], which were widely used in such heavy-ion experiments as ALICE, PHENIX, STAR, HADES and is planning the TOF CBM. Such widespread use of this detector caused by that the multigap resistive plate chamber has good timing characteristics. At the same time, the MRPC is quite easy to manufacture and it is relatively inexpensive. Its production requires materials that are commercially available.

The multigap resistive plate chamber consists of a stack of resistive plates separated one from the other with equal size spacers creating a series of gas gaps. High voltage coating is made on the outer surfaces of the outer resistive electrodes. Internal plates are left electrically floating. The voltage of the internal plates appears due to the flow of electrons and ions created in the gas gap. The resistive electrodes quench the streamer and prevent a spark breakdown. The MRPC operates at high gain in avalanche mode. Float glass plates are used as resistive plate electrodes.

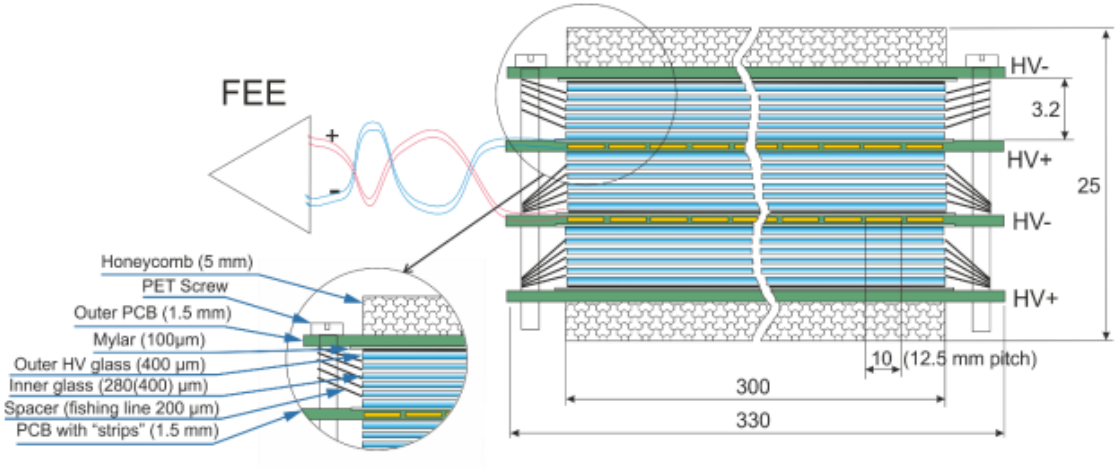

Fig. 2.1. Scheme of the triple-stack MRPC with strip readout for TOF MPD

A scheme of the MPD TOF detector is presented in Fig. 2.1. The detector consists of three stacks of 5 gas gaps each. As resistive electrodes is used common float glass. The outer glass electrodes have the thickness of 400 μm. The internal glass electrodes have the thickness of 270 μm. The fishing line as a spacer defines the 200 μm gap between the all resistive electrodes. The outer part of external glass electrodes is covered by the conductive paint with surface resistivity about 2 – 10 MΩ/□ to apply

high voltage. Dimensions of the resistive glass are 300 x 640 mm^2. It defines a surface of active area of one MRPC.

Similar construction has the ToF-400 system using in BM@N detector. The main difference between the MRPC using in BM@N and MPD detector is number of strips, BM@N has 48 and MPD 24 strips, respectively. The ToF-400 system consists of two parts (left and right) that are placed symmetrically to a beam. Each part consists of two gas boxes each content 5 MRPCs. The active area of the MRPCs overlap on 50 mm inside the box. Overlap of the gas boxes ensures crossing of the active area of detectors for 50 mm. The size of each part is 1.15x1.3 m^2 and defined to suffice the geometrical acceptance of the tracking detectors. Separation of pions/kaons up to 3 GeV/c requires time resolution better than 80 ps for the ToF-400 detectors.

3. Readout electronics

3.1 Front-end electronics based on the NINO ASIC

Readout electronics for the MPD-TOF consist of the front-end electronics (FEE) and data acquisition system (DAQ). Was decided to use electronics like used in the TOF ALICE. Since each detector of MPD has a 24 strip it was decided to create a 24-channel amplifier on the example of the front-end board of the TOF ALICE based on the NINO ASIC [3].

The NINO application-specific integrated circuit (ASIC) (Fig. 3.1) developed in 0.25 micron CMOS technology recently by the CERN LAA project, which combines a fast amplifier, discriminator and stretcher. The NINO ASIC had to satisfy the following requirements: differential input; optimized to operate with 30-100 pF input capacitance; LVDS differential output; output pulse width dependent on the charge of the input signal; fast amplifier to minimize time jitter (a peaking time less than 1 ns); threshold of discriminator adjustable in the range 10 –100 fC; eight channels per ASIC. Main features of the NINO ASIC are shown in Table 3.1.

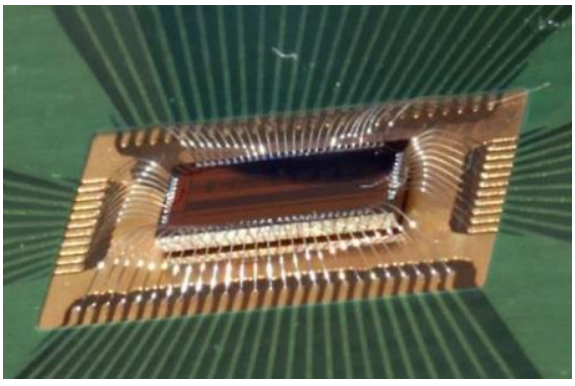

Fig. 3.1. The NINO ASIC (8 channels) directly bonded on the PC board (no packaging).

Table 3.1. NINO ASIC specifications table.

Parameter	Value
Number of channels	8
Peaking time	1 ns
Supply voltage	2.5 mV
Power consumption	27mV/ch
Input signal range	30 fC - 2 pC
Noise (with detector)	< (2.5 - 5) x 10^3 e- rms
Discriminator threshold	10 fC to 100 pC
Differential input impedance	40 Ω < Z_{in} < 75 Ω
Timing precision	< 10ps jitter
Outputs	LVDS

For the TOF MPD the 24-channel NINO based preamplifier board was developed (Fig. 3.2). This preamplifier board is adapted for the two-side strip readout in MRPC at the MPD experiment. Overall dimensions of the preamplifier are 196.5 x 89 mm^2.

Features of the MPD TOF preamplifier board:

- stabilized voltage supply of the NINO;
- the input impedance matched to impedance of the MRPC;
- overload protection at input channels;
- capacitors at the inputs for two-side strip readout;
- the possibility to use as a trigger (parallel “or” output);
- the threshold monitoring and control;
- the NINO’s voltage monitoring and control;
- the board and the gas space thermal monitoring.

Fig. 3.2. 24-channel NINO based preamplifier board with the CXP output connector.

3.2 The prototype of analog front-end electronics

As alternative was developed an analog front-end electronics (FEE) for the ToF system (Fig. 3.3). The prototype of amplifier consists in AD4960 differential amplifier and ADA4937 differential repeater for matching with the cable, that contains 12 amplification channels. For this all channels were numbered as shows in Fig. 3.4. It has a bandwidth of 1 GHz. To collect data was coupled an analog-digital converter DRS4 (Fig. 3.5). It has 4 input channels for analog signals, the ability to connect an external trigger signal and a synchronization signal, as well as a USB interface for connecting to a computer. Using the DRSOsc program [4], the computer can serve as an oscilloscope and record the incoming data for further processing.

Fig. 3.3. Amplifier board.

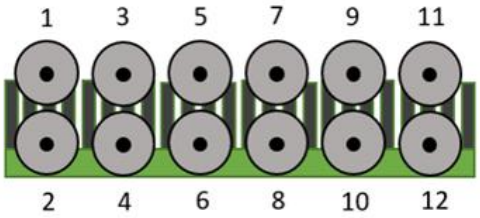

Fig. 3.4. Schema of channels out numbered

Fig. 3.5. DRS4 board.

4. Realization and methods

4.1 Calibration of analog readout system

The calibration was made channel by channel, to correctly interpret the data. Were supplied five different amplitudes between 15 - 100 mV as input amplitude and two amplifiers were used. A gain ~7 was expected. The scheme of the calibration stand is shown in Fig. 4.1.

The Fig. 4.2 and 4.3 show the fitted curves resulting from the calibrations for both amplifiers. We used the linear fit with the form $Amp_{out} = p0 + p1 * Amp_{in}$, the coefficients p0 and p1 can be found in figures. All acquired data processing was done in ROOT code [5].

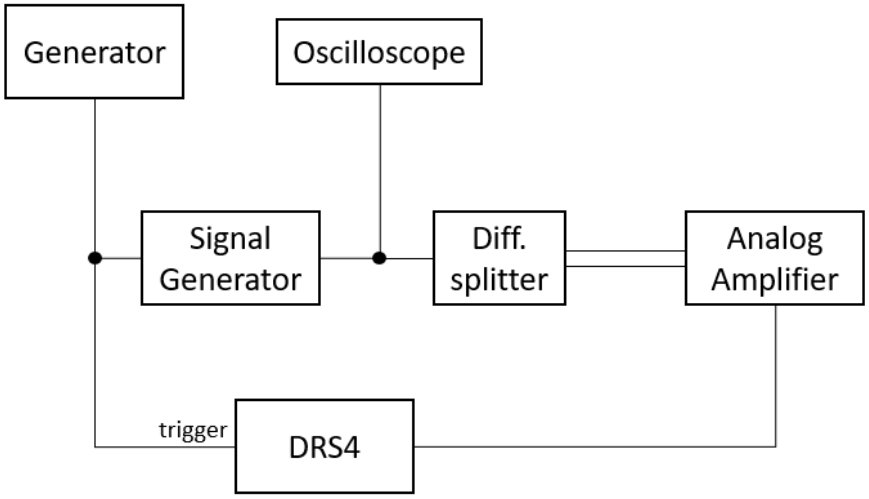

Fig. 4.1. The scheme of the calibration stands.

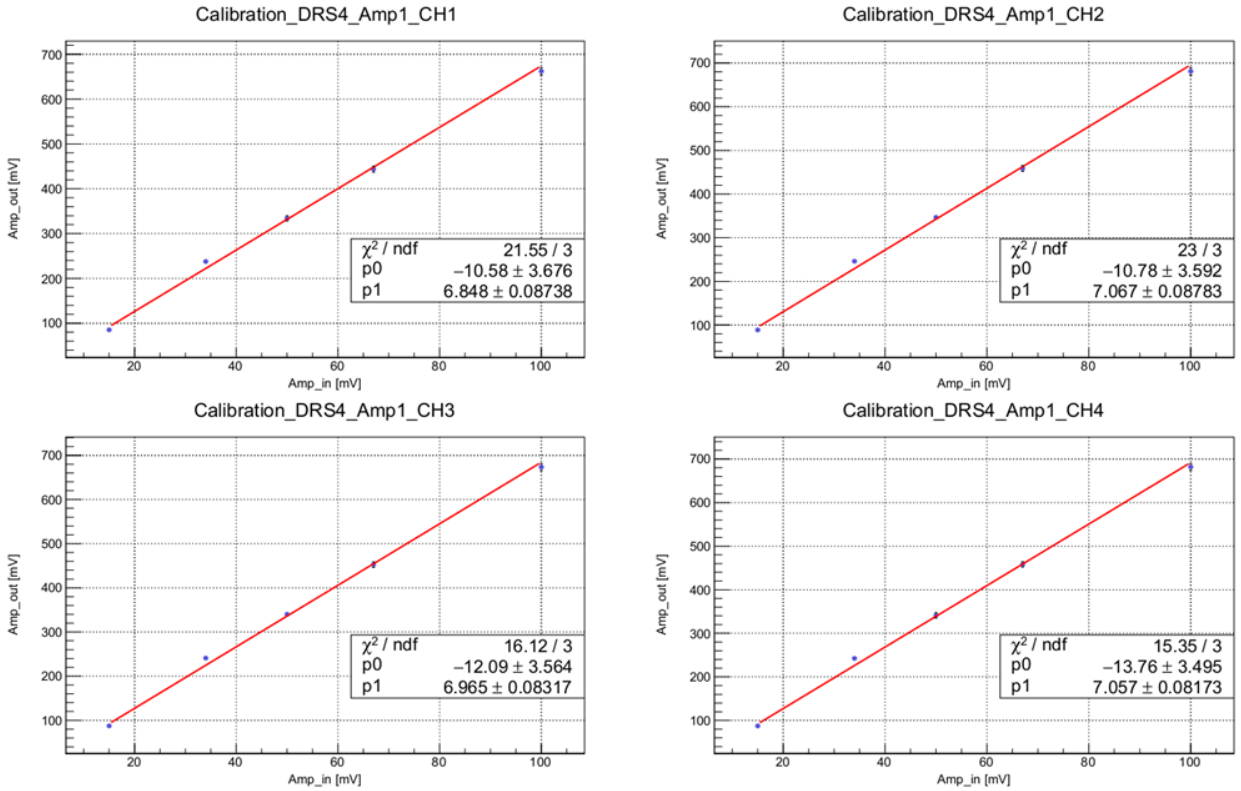

a

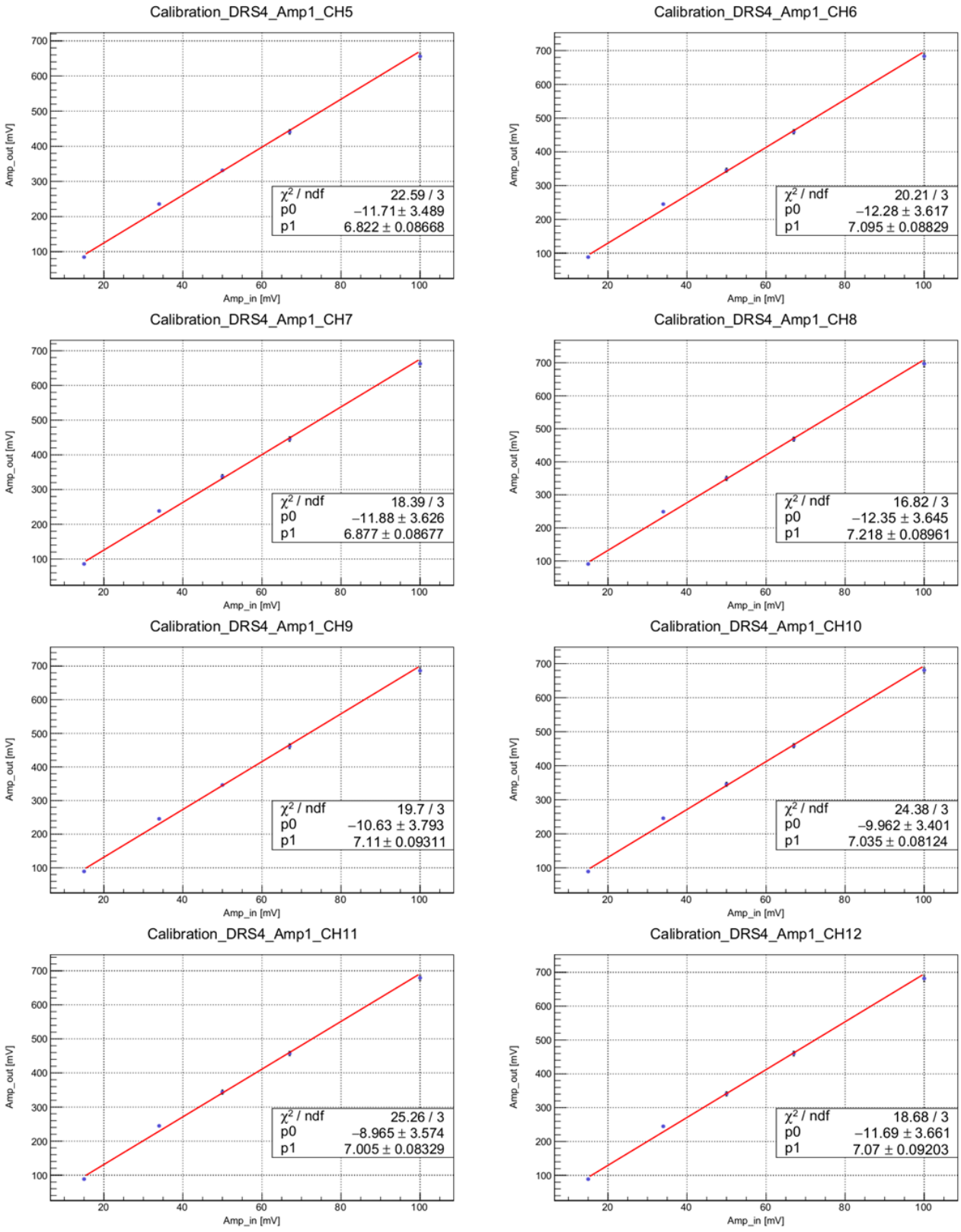

b

Fig. 4.2. Amplitude calibration of 12 channels of amplifier 1; a) channels 1 - 4 & b) channels 5 – 12.

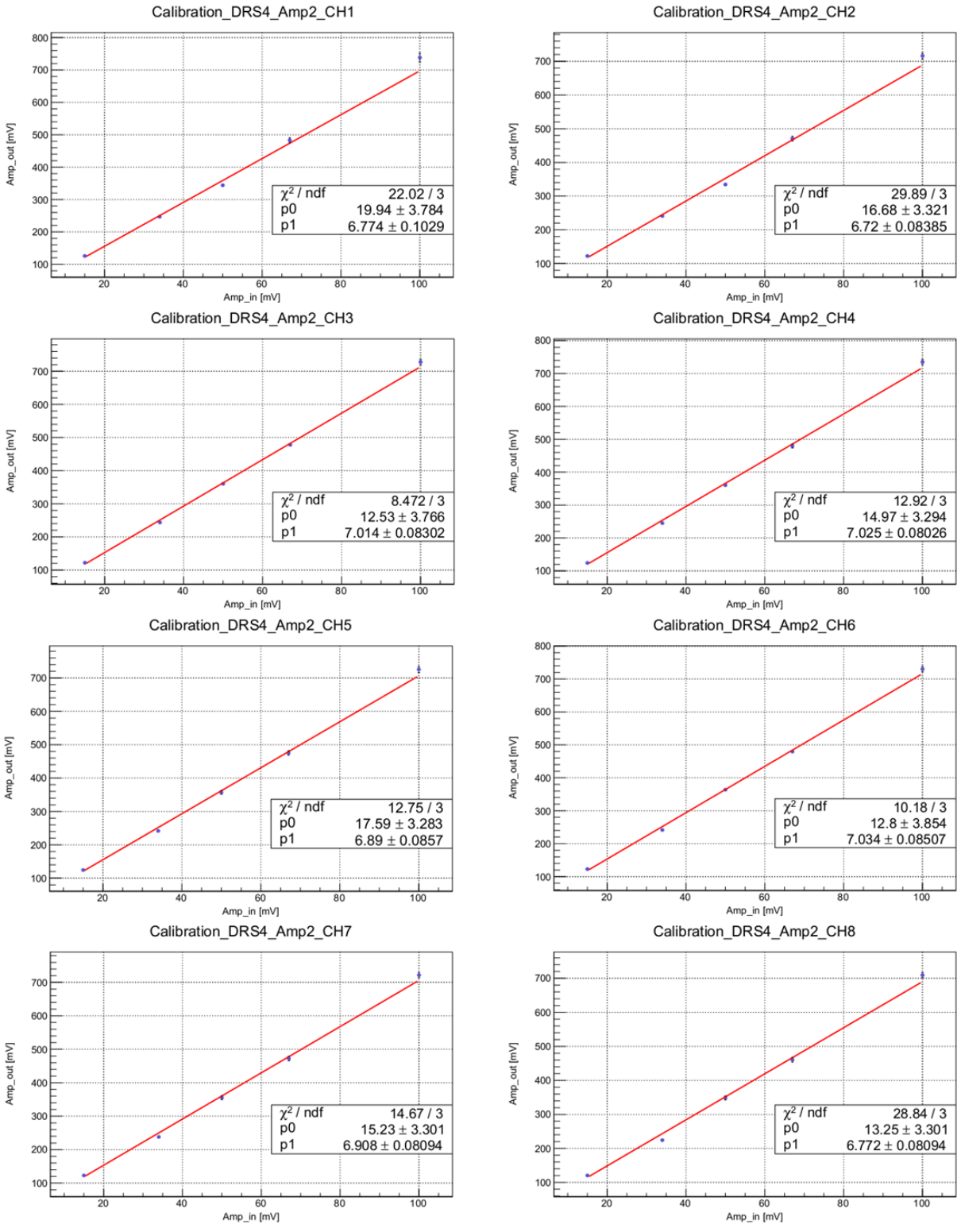
Calibration_DRS4_Amp2_CH1
χ² / ndf 22.02 / 3
p0 19.94 ± 3.784
p1 6.774 ± 0.1029
Calibration_DRS4_Amp2_CH2
χ² / ndf 29.89 / 3
p0 16.68 ± 3.321
p1 6.72 ± 0.08385
Calibration_DRS4_Amp2_CH3
χ² / ndf 8.472 / 3
p0 12.53 ± 3.766
p1 7.014 ± 0.08302
Calibration_DRS4_Amp2_CH4
χ² / ndf 12.92 / 3
p0 14.97 ± 3.294
p1 7.025 ± 0.08026
Calibration_DRS4_Amp2_CH5
χ² / ndf 12.75 / 3
p0 17.59 ± 3.283
p1 6.89 ± 0.0857
Calibration_DRS4_Amp2_CH6
χ² / ndf 10.18 / 3
p0 12.8 ± 3.854
p1 7.034 ± 0.08507
Calibration_DRS4_Amp2_CH7
χ² / ndf 14.67 / 3
p0 15.23 ± 3.301
p1 6.908 ± 0.08094
Calibration_DRS4_Amp2_CH8
χ² / ndf 28.84 / 3
p0 13.25 ± 3.301
p1 6.772 ± 0.08094
Amp_out [mV]
Amp_in [mV]

a

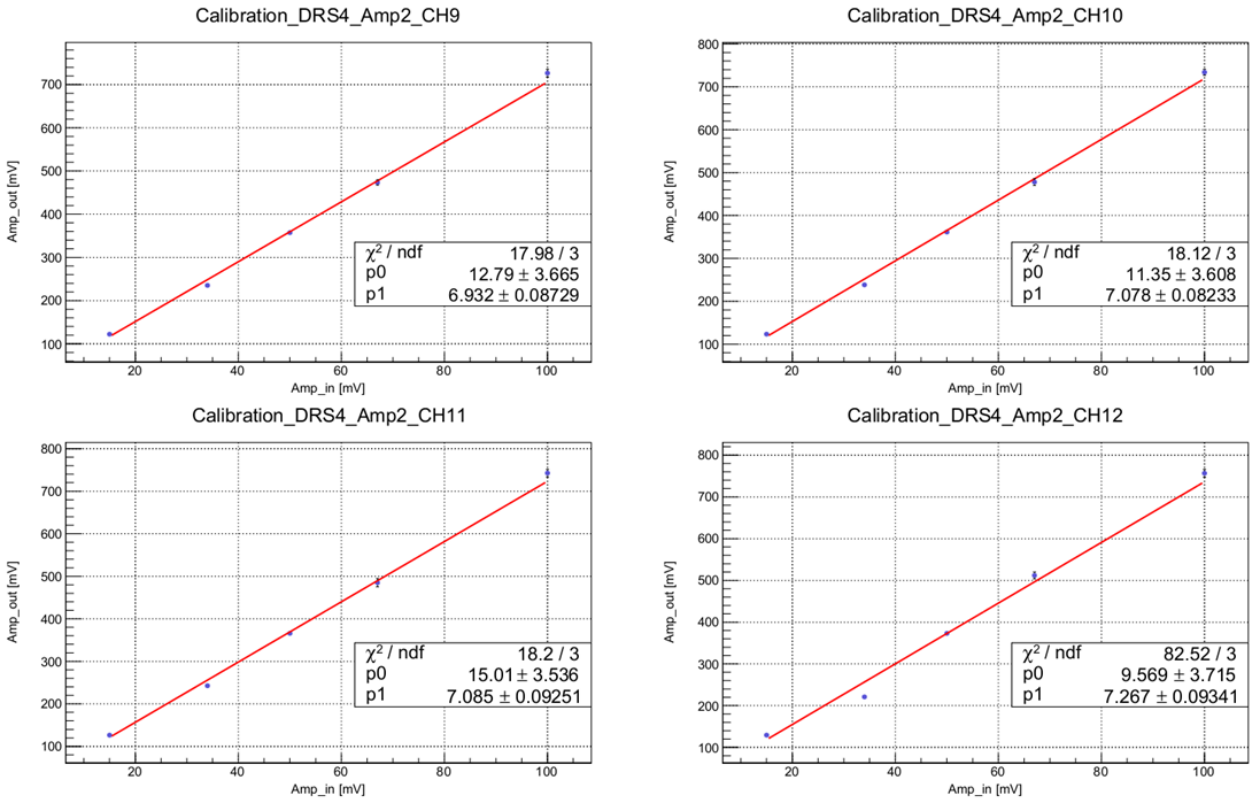

b

Fig. 4.3. Amplitude calibration of 12 channels of amplifier 2; a) channels 1 - 8 & b) channels 9 – 12.

4.2 Detector test setup

The setup used for test analog readout with cosmic rays was MRPC enclosed in a sealed aluminum box filled with a gas mixture of 90% tetrafluoroethane ($C_2H_2F_4$), 5% isobutene (i-C_4H_{10}) and 5% sulfur hexafluoride (SF_6) at atmospheric pressure. The detector was putted inside the chamber on plastic legs and fixed to them with screeds and plastic bolts. Transition plates are glued into the gas box, which allows the signals to be discharged outside. The camera itself is assembled from aluminum plates on bolts and sealant, and on top of the perimeter is laid an elastic rubber seal, to which the screws are pressed down by tightening the cover. Overall dimensions of the detector (600x300 mm^2) are determined by the size of the glass. 48 pickup electrodes with pitch of 12.5 mm look like strips and made at the inner layer of the PCB.

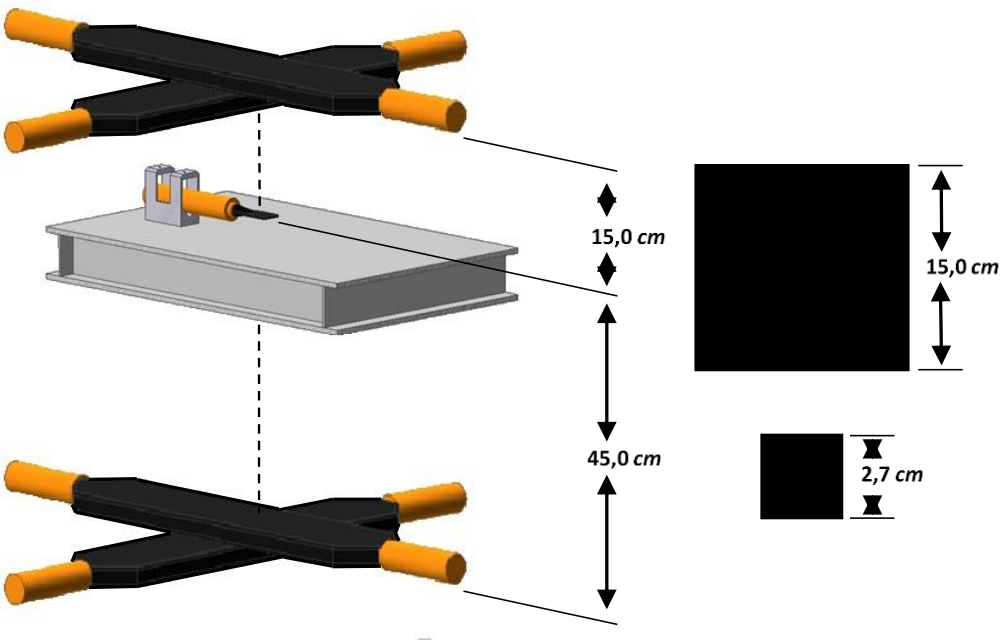

Fig. 4.4. Schema of setup with length details (Black squares are a geometric section of scintillator)

In test, 4 channels of detector were taken, 2 channels per strip, and the signal from a scintillators array was used as the trigger. A scheme, details and description of this setup are shown in Fig. 4.4, the black ones are scintillators. When a charged particle hits the scintillator from a scintillating substance, a photon is knocked out, which is trapped by the photocathode, converted into a current pulse in it, and amplified by a system of dynodes. Since the area of the working surface of the scintillator is smaller than that of the MRPC, the particles were detected much less frequently. Data were recorded on Raspberry Pi via DRS4.

The four channels of the DRS4 were coupled in the following way with the amplifier's channels: channels 1 and 2 of amplifier 1 with channel 1 and 3 of DRS4, and channels 1 and 2 of amplifier 2 with channel 2 and 4 of DRS4, respectively.

Was calculating the solid angle of this setup in order to know the number of particles that could activate the trigger. The solid angle result was $\Omega \approx 0.2256$ sr and number of particles 0.0182 min^{-1} cm^{-2} approximately.

The Fig. 4.5 shows the waveform of one event for the 4 channels after making the decode [4] of data taking. The red line is the baseline of the signal fitted between - 190 and - 100 ns.

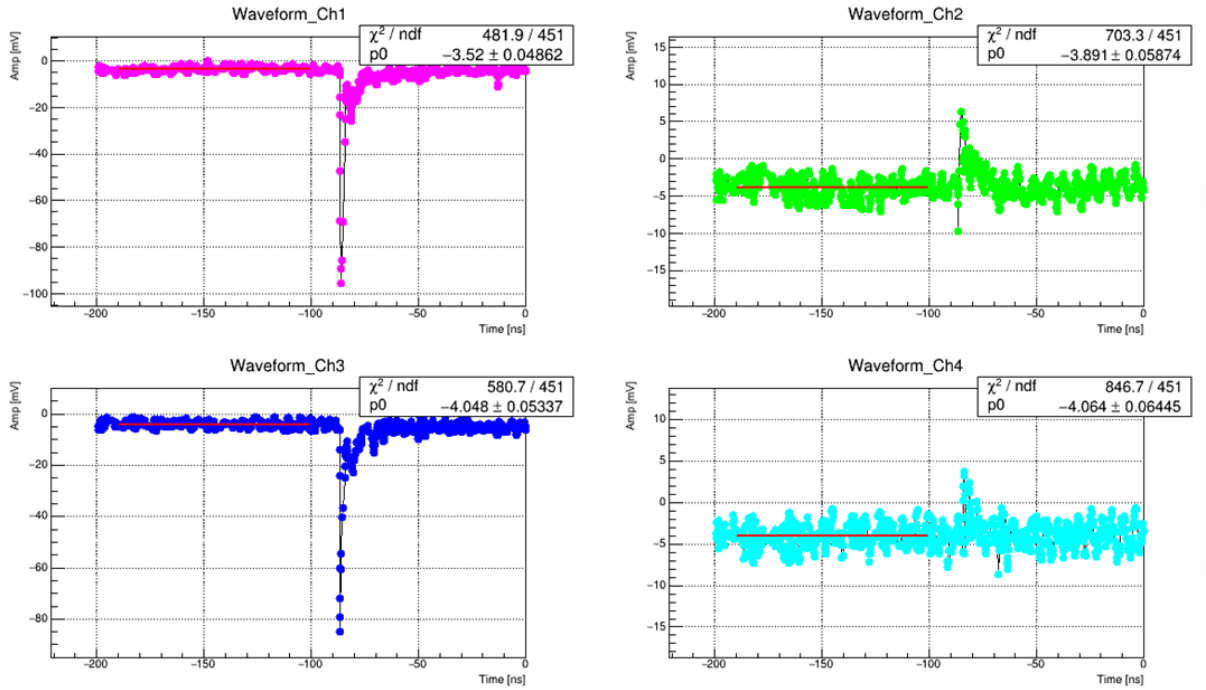

Fig. 4.5. Waveform made from data taking of one event.

5. Results

Firstly, we analyze the absolute maximum value of the output amplitude. For this, we use baseline as can be seen in Fig. 4.5 and calculate $|Amp_{min} - Amp_{baseline}|$. The histograms for this magnitude were fitted by a Landau distribution, the fits are shown in Fig. 5.1.

The most probable values obtained from the fits are 13.61, 13.66, 13.47 and 13.94 mV for each DRS4 channel, respectively. The resultant spectra do not coincide with the expected ones because, as can be seen in Fig. 4.5, the amplitude of our signal should be around 90 mV. This means that the peak observed in the spectrum corresponds to signal noise.

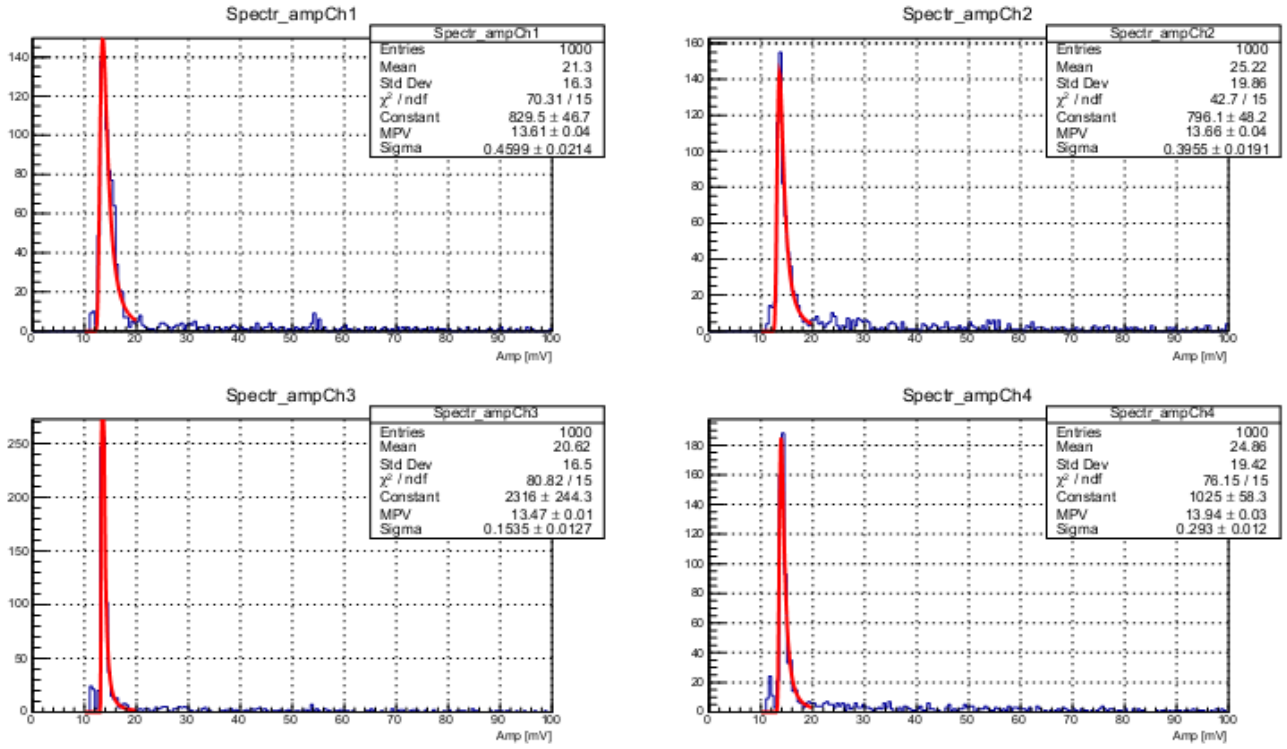

Fig. 5.1. Spectra of absolute maximum amplitude for each DRS4 channels.

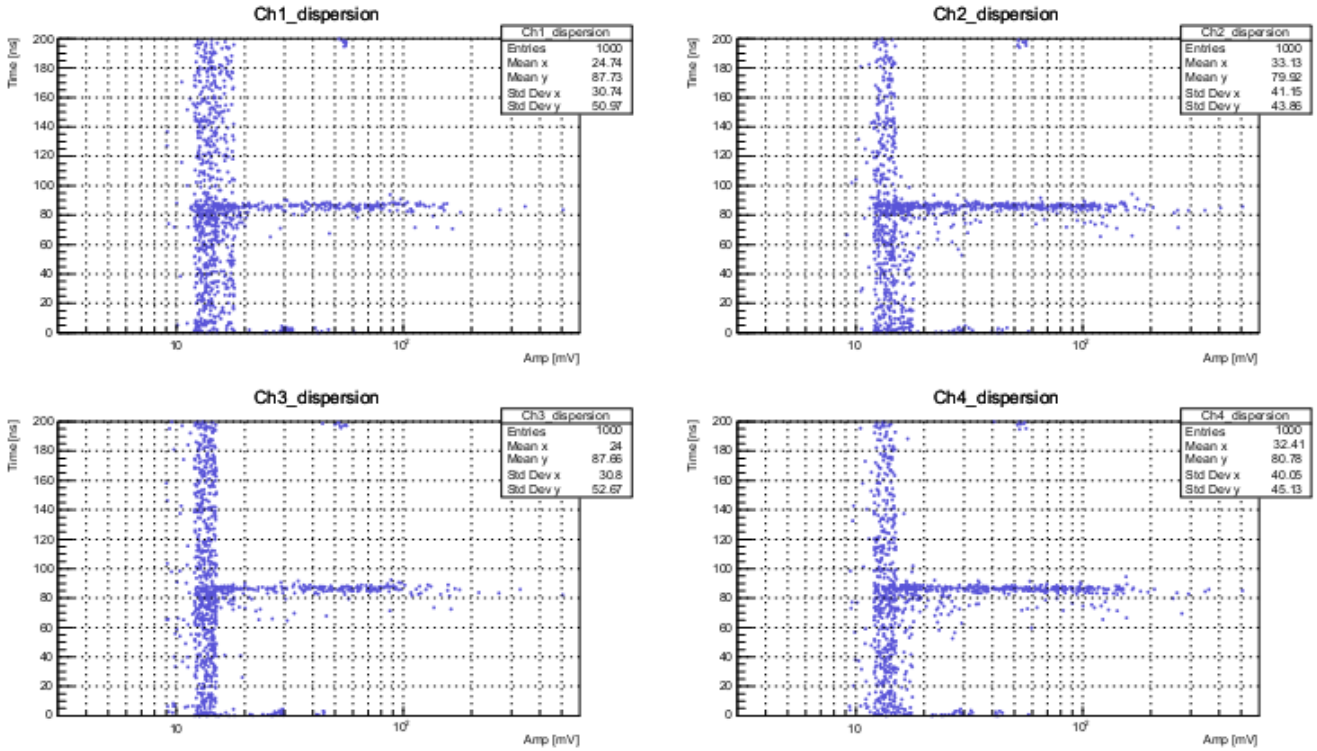

Fig. 5.2. Spectra of dt vs absolute maximum amplitude for each channel.

Finally, scatter histograms were made from dt vs absolute maximum amplitude (Fig. 5.2) in order to check the temporal distribution of the absolute maximum amplitude of signal. Was made a

projection on X plane for channel 1 (Fig. 5.3) and confirmed the results for amplitude spectra, the peak of ~13 mV is noise signal.

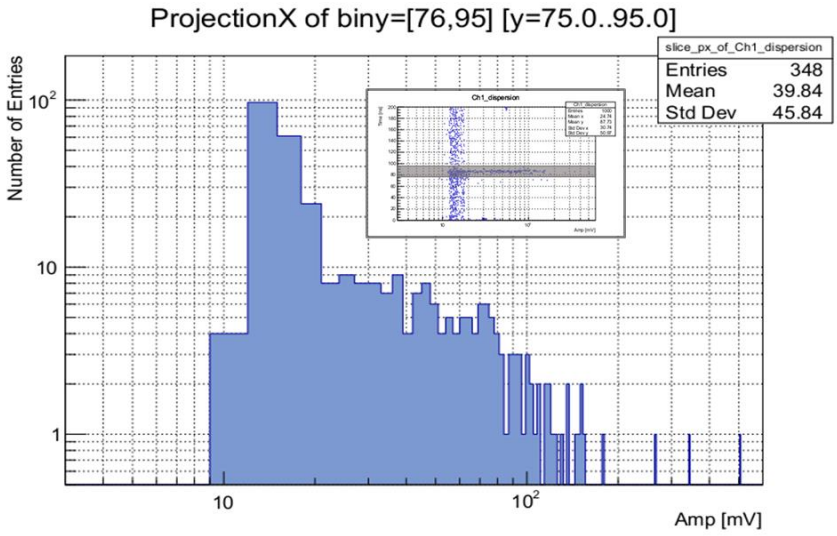

Fig. 5.3. X plane projection of channel 1 dispersion.

The minimum charge that can be registered by this FEE was also determined. For this was used the minimum amplitude induced in the strip without noise, the definition of charge current and Ohm's law. The final equation is:

$$q = \frac{V_{in} * t}{R},$$

it was calculated for t = 2 ns and R = 50 Ω and result equal to 170 fC.

6. Conclusions

The new prototype of analog FEE was calibrated and then tested with cosmic rays. The calibration was carried out channel by channel of 12 channels for 2 amplifiers. In the cosmic rays test, the absolute maximum value of the output amplitude histograms was made, verifying that spectra do not coincide with the expected ones because the amplitude of our signal should be around 90 mV and in spectra only can see a peaks of ~13 mV. This means that the peaks observed in spectra corresponds to signal noise. This fact was checked with scatter histograms and X plane projection of that histograms. But, on the other hand, it was determined that the minimum charge that can be registered in the detector is 170 fC approximately. The following version of this amplifier is being developed and a gain of 25 is expected.

7. References

[1] Conceptual Design Report. The MultiPurpose Detector – MPD to study Heavy Ion Collisions at NICA. Version 1.4. (http://mpd.jinr.ru/wp-content/uploads/2016/04/MPD_CDR_en.pdf)

[2] NICA web page (http://nica.jinr.ru)

[3] MPD NICA Technical Design Report of the Time of Flight System (TOF) (http://mpd.jinr.ru/wp-content/uploads/2017/05/TDR_TOF_20_04_2017.pdf)

[4] DRS4 Evaluation Board User's Manual. Version 5.1 (https://www.psi.ch/drs/DocumentationEN/manual_rev51.pdf)

[5] ROOT - CERN. An object oriented framework for large scale data analysis (https://root.cern.ch)